

Fe₂O₃ and Gd₂O₃ Nanoparticles Embedded in Mesoporous Silica: Magnetic Properties Comparison

O. KAPUSTA^{a,*}, A. ZELENÁKOVÁ^a, P. HRUBOVČÁK^a, V. GIRMAN^a AND V. ZELENÁK^b

^aInstitute of Physics, Faculty of Sciences, P.J. Šafárik University, Park Angelinum 9, 041 54 Košice, Slovakia

^bInstitute of Chemistry, Faculty of Sciences, P.J. Šafárik University, Moyzesova 11, 040 01 Košice, Slovakia

Nanocomposite materials containing Fe₂O₃ and Gd₂O₃ nanoparticles with the same concentration were prepared by nanocasting method. At this procedure silica matrix serves as nanoreactor for growth of nanoparticles. Temperature and external dc field dependences of the magnetization both samples were compared. Composite containing Fe₂O₃ nanoparticles shows superparamagnetic behaviour with blocking temperature around 45 K. Otherwise, paramagnetic properties were observed for the sample with Gd₂O₃ (above 10 K). Additionally, due to free pores the silica matrix could serve as medium to increase the number of bonded water molecules. These properties together with appropriate magnetic characteristics make studied materials suitable for magnetic resonance imaging applications.

DOI: [10.12693/APhysPolA.131.860](https://doi.org/10.12693/APhysPolA.131.860)

PACS/topics: 07.78.+s, 47.11.Kb, 75.75.Cd, 75.40.Cx, 78.20.-e

1. Introduction

In last years, there is an effort to improve contrast agents for magnetic resonance imaging (MRI), which enhance the contrast between healthy and diseased tissue by increasing the image quality and sensitivity of the method [1]. Generally, there are two different classes of MRI contrast agents. T_1 contrast agents are reducing proton relaxation time and providing positive contrast (bright signal) and T_2 contrast agents are shortening the proton transverse relaxation time thereby they are causing negative contrast (dark signal) [2]. Positive contrast agents are typically of paramagnetic nature e.g. gadolinium complexes, while superparamagnetic materials, mainly based on iron oxide nanoparticles, are negative contrast agents. To be effective, MRI contrast agents must have a strong effect on longitudinal and transverse relaxation rate of water proton. To design the contrast agent two parameters are usually considered, increasing the rotational correlation time by increasing molecular weight and size or increasing the number of coordinated waters. Modified mesoporous silica could be excellent medium how to prepare MRI contrast agents. Due to porous structure of the silica, water can freely move in and out of the matrix and simultaneously, it can be carrier of metal nanoparticles. Additionally, the nontoxic silica can be easily derived and targeted contrast agents can be synthesized [3].

In our work we prepared and compared nanocomposite consisting of Gd₂O₃ and Fe₂O₃ nanoparticles embedded in the hexagonal mesoporous silica matrix SBA-15 with the same concentration. We studied structural, magnetic, optical and hydrodynamic properties and we discuss their potential use as MRI contrast agents.

2. Experimental

Mesoporous silica SBA-15 was synthesized according to Zhao et al. [4] and modified by iron or gadolinium oxides via wet-impregnation method, where the mesoporous silica acts as a hard template for growth of the nanoparticles. 250 mg SBA-15 was dispersed into 0.5 M solution of Fe(NO₃)₃ · 9H₂O or Gd(NO₃)₃ · 6H₂O with ultrasonication during 30 min at 320 K. After impregnation, samples were dried and calcinated at 770 K 5 h in air atmosphere. The sample containing Fe₂O₃ was denoted as Fe@SBA-15 and Gd₂O₃ as Gd@SBA-15. The size and morphology of samples were investigated by transmission electron microscope JEOL 2100. The magnetic measurements were performed on a commercial SQUID-based magnetometer (Quantum Design MPMS 5 XL) over temperature range (2–300 K) and applied magnetic field (up to 50 kOe). Optical properties were characterized by UV-VIS spectrometer Spectra 2500. Hydrodynamic properties dependences on pH (Zeta potential and hydrodynamic diameter) were carried out by Zetasizer Nano-ZS (Malvern) and MPT-2 Autotitrator (Malvern). The sample dispersions in 0.001 M NaOH with concentration 0.28 g/l were titrated by 0.5 M HCl in a wide pH range (9.8–2.0).

3. Result and discussion

The prepared composite samples were structurally characterized by transmission electron microscopy (TEM), energy dispersive X-ray spectroscopy (EDX) and X-ray adsorption near edge structure (XANES). TEM micrographs (Fig. 1) of composites revealed retained hexagonal symmetry of porous matrices after loading and crystallization of Gd₂O₃ and Fe₂O₃ nanoparticles. The size of the silica matrix was approximately 7 nm. XANES spectra as well as EDX measurement confirmed the presence of Gd₂O₃ and α -Fe₂O₃ [5]. The EDX spectra showed the atomic M/Si (M = Fe, Gd) ratio around 0.12, which represents \approx 15 wt%. Nanoparticles inside pores were close

*corresponding author; e-mail:
ondrej.kapusta@student.upjs.sk

to spherical shape with size up to 7 nm. The detailed structural study was described elsewhere [6, 7].

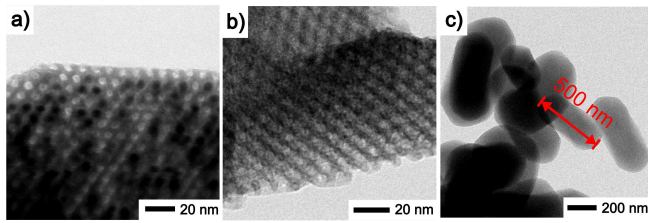


Fig. 1. TEM micrographs: (a) Fe@SBA-15 (cross-section), (b) Gd@SBA-15 (cross-section), (c) silica particles.

The magnetic properties of composites were investigated using the measurements of field- and the temperature-dependences of magnetization. The magnetization dependence on the external magnetic field of Fe@SBA-15 at 2 K exhibits coercivity $H_C \approx 2400$ Oe (Fig. 2) while $M(H)$ dependences measured at 50 and 300 K do not show coercivity.

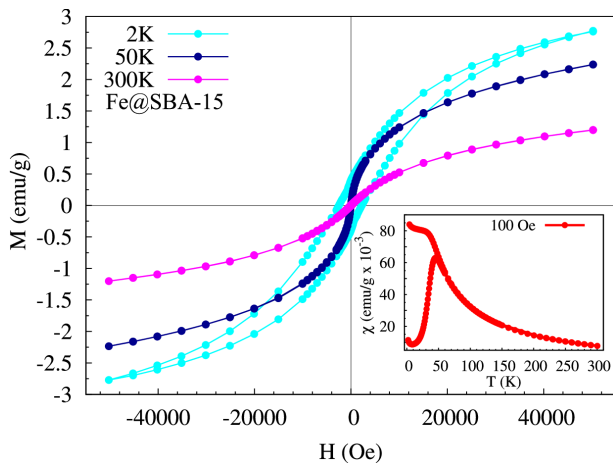


Fig. 2. $M(H)$ dependence of the sample Fe@SBA-15 at given temperatures. Inset shows $\chi(T)$ dependence.

We have measured the temperature dependence of magnetization in zero field cooled/field cooled (ZFC/FC) regimes at external magnetic field 100 Oe. The presence of a maximum in the ZFC curve corresponds to blocking temperature $T_B \approx 45$ K. Above blocking temperature ZFC and FC curves are merged. System is in superparamagnetic state, where magnetic moments can freely fluctuate and coercivity was not observed ($M(H)$ curves at 50 and 300 K). Below T_B magnetic moments are blocked in the external magnetic field direction and coercivity appeared. Additionally, sample shows peculiar behaviour in low temperature region (2–10 K), which predicts additional freezing process. We will provide detailed study of this process in the future investigations.

On the other hand, the sample Gd@SBA-15 with the same nanoparticle concentration as sample Fe@SBA-15

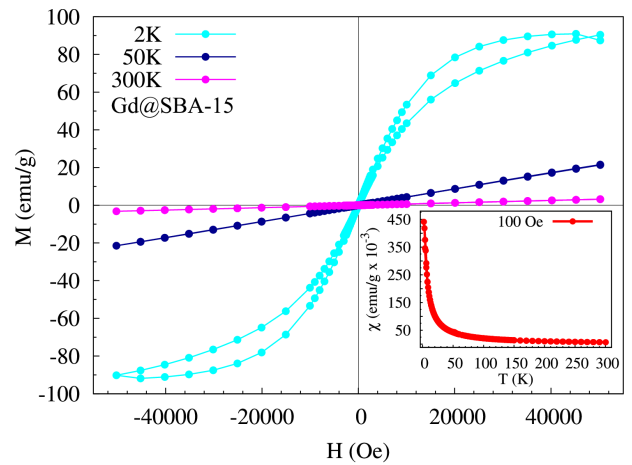


Fig. 3. $M(H)$ dependence of the sample Gd@SBA-15 at given temperatures. Inset shows $\chi(T)$ dependence.

shows paramagnetic behaviour in temperature range 10–300 K, which is confirmed by measured $M(H)$ curves (Fig. 3). ZFC and FC curves are irreversible below temperature 10 K. This nontypical paramagnetic behaviour confirms the $M(H)$ curve measured at 2 K (Fig. 3). The curve is irreversible at external magnetic field in range 2–50 kOe. These observations predict the presence of magnetization processes induced by external magnetic field. Also this phenomenon will be the subject of our future research. A comparison of the magnetic properties shows that both prepared composites do not exhibit hysteresis at 300 K, however saturation magnetization is higher $M_S \approx 3.2$ emu/g for Gd@SBA-15 (at 50 kOe) than $M_S \approx 1.2$ emu/g for Fe@SBA-15. Magnetic moment value shows opposite trend. While magnetic moment of Gd@SBA-15 (obtained by distribution Langevin functions fit) is $27.8 \mu_B$, its value in the case of the sample Fe@SBA-15 is much higher and is $270.4 \mu_B$. These properties show on different magnetization processes in both investigated samples. Whereas Fe_2O_3 nanoparticles show superparamagnetic relaxation of magnetic moments at room temperature, typical Curie paramagnetic relaxation is present in Gd_2O_3 nanoparticles.

Subsequently, the prepared samples were examined in solution. The optical properties were analysed by UV-VIS spectroscopy for detection possibility. The absorption spectrum is presented in Fig. 4. Typically, Gd_2O_3 nanoparticles show a very weak broad peak at ca. 325 nm [8] although one would expect some sharp peaks due to many unpaired electrons of Gd. From experience, however, it is known that Gd^{III} compounds has very light pink colour. This peak was not observed in the spectrum which could be caused by the matrix walls, which damped signal. Compared to Gd, sample containing Fe has reddish colour and broad peak around 400 nm was observed in the UV-VIS spectra. This spectrum is consistent with the colour of the sample and the observed spectra for Fe_2O_3 . The optical properties show that only

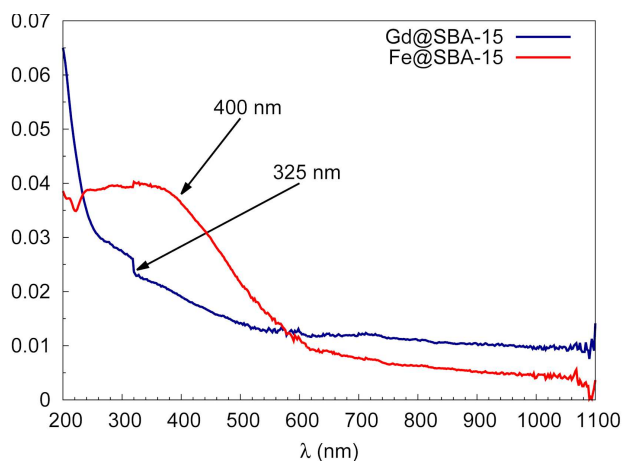


Fig. 4. UV-VIS spectra of the studied samples.

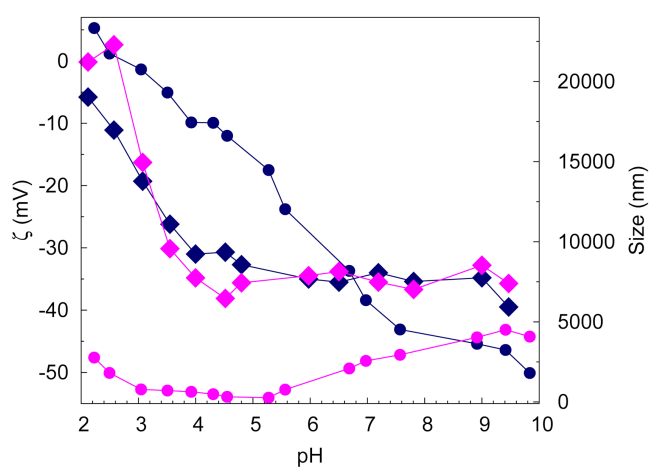


Fig. 5. Hydrodynamic diameter (right, magenta) and zeta potential (left, dark blue) profiles of the samples Gd@SBA-15 (circles) and Fe@SBA-15 (rhombuses) at different pH values.

the sample Fe@SBA-15 can be detected in the UV-VIS light region.

The dispersions of the samples were investigated by dynamic light scattering (DLS) and electrophoresis methods in the solution at different values of pH. DLS was used to determine the hydrodynamic diameter and electrophoresis was used to determine zeta potential. The measured dependences are displayed in Fig. 5. The samples behave very differently in solution. The sample Fe@SBA-15 has strong coherence between hydrodynamic diameter and zeta potential, which is indicated by the similar pattern of both curves. Hydrodynamic diameter and zeta potential change very little in pH range 9.8–4.0. Low composite mobility reflects the high value of hydrodynamic diameter ≈ 8000 nm. Good dispersion stability confirms zeta potential value, which is ≈ -35 mV in this pH region. Below pH = 4.0 dispersion stability expires.

Approximately linear decrease of zeta potential was observed for Gd@SBA-15. Composite is stable in pH range 9.8–6.7, where zeta potential is in range (–50)–(–34) mV. The hydrodynamic diameter decreases in this pH range, in pH range 5.5–3.0 is slightly different and again raises below pH = 3.0. Observed hydrodynamic diameter or zeta potential dependences show a correlation between them and sample composition. However, decrease of zeta potential below pH = 4.0 indicates significant impact of silica matrix OH surface groups on nanoparticles charge.

4. Conclusions

We have prepared Fe₂O₃ and Gd₂O₃ nanoparticles with the same concentration embedded into channels of mesoporous silica matrix SBA-15. Structural methods confirmed the presence of oxides allocated within the silica pores. Observed magnetic characteristic show paramagnetic nature of Gd@SBA-15 and superparamagnetic nature of Fe@SBA-15. Both samples do not exhibit hysteresis at 300 K. Detection opportunity in UV-VIS range shows only the sample containing iron oxide nanoparticles. Prepared samples are stable in wide range of pH (9.8–6.6) which includes pH of blood ≈ 7.4 . Studied composites could be applied as negative (with Fe) and positive (with Gd) contrast agents for MRI. Moreover, matrix serves not only as nanoreactor for size and growth control of nanoparticles but also serves as medium to increase number of bonded water molecules.

Acknowledgments

This work was supported by the Slovak Research and Development Agency under the contracts APVV-520-15, the VEGA projects (No. 1/0377/16, No. 1/0745/17) and to VVGS-PF-2016-72646 project. The authors (A.Z. and V.Z.) would like to thank DESY/HASYLAB project under No. I-20110282 EC.

References

- [1] D. Niu, X. Luo, Y. Li, X. Liu, X. Wang, J. Shi, *Appl. Mater. Interf.* **5**, 9942 (2013).
- [2] S. Santra, S.D. Jativa, C. Kaittanis, G. Normand, J. Grimm, J.M. Perez, *ACS Nano* **8**, 7281 (2012).
- [3] Y.-S. Lin, Y. Hung, J.-K. Su, R. Lee, C. Chang, M.-L. Lin, C.-Y. Mou, *J. Phys. Chem. B* **108**, 15608 (2004).
- [4] D. Zhao, Q. Huo, J. Feng, B.F. Chmelka, G.D. Stucky, *J. Am. Chem. Soc.* **120**, 6024 (1998).
- [5] V. Zelenak, A. Zelenakova, J. Kovac, U. Vainio, *Nanocasting of Gd₂O₃ in porous silica matrix*, DESY, annual report file, Hamburg 2011.
- [6] V. Zelenak, A. Zelenakova, J. Kovac, U. Vainio, N. Murafa, *J. Phys. Chem. C* **113**, 13045 (2009).
- [7] A. Zelenakova, O. Kapusta, V. Zelenak, *Acta Phys. Pol. A* **126**, 218 (2014).
- [8] S.A. Khan, S. Gambhir, A. Ahmad, *Beilstein J. Nanotechnol.* **5**, 249 (2014).